RSC Advances

RSC Publishing

PAPER

View Article Online
View Journal | View Issue

Fabrication of Au/Pd alloy nanoparticle/*Pichia pastoris* composites: a microorganism-mediated approach

Cite this: *RSC Advances*, 2013, **3**, 15389

Huimei Chen,[a] Daohua Sun,[bc] Xinde Jiang,[bc] Xiaolian Jing,[a] Fenfen Lu,[bc] Tareque Odoom-Wubah,[bc] Yanmei Zheng,[b] Jiale Huang*[bc] and Qingbiao Li[abcde]

Received 13th March 2013,
Accepted 21st June 2013

DOI: 10.1039/c3ra41215f

www.rsc.org/advances

Synthesis of metal nanoparticles (NPs) is in the limelight in modern nanotechnology. In this present study, bimetallic Au/Pd NP/*Pichia pastoris* composites were successfully fabricated through a one-pot microbial reduction of aqueous $HAuCl_4$ and $PdCl_2$ in the presence of H_2 as an electron donor. Interestingly, flower-like alloy Au/Pd NP/*Pichia pastoris* composites were obtained under the following conditions, NaCl concentration 0.9% (w/v), molar ratio of Au/Pd (1 : 2) and the time for pre-adsorption of Au(III) and Pd(II) ions 15 min, through fresh yeast reduction. The mapping results from scanning transmission electron microscopy (STEM) with a high-angle annular dark field detector confirmed that the Au/Pd NPs on the surface of the yeast were indeed alloy. Furthermore, the energy dispersive X-ray (EDX) and X-ray photoelectron spectroscopy (XPS) measurements showed that the composition of the bimetallic NPs were consistent with the initial molar ratio of the precursors.

1. Introduction

Metal nanostructures are attractive for a variety of applications ranging from catalysis to photonics due to the enhancement of properties achieved at the nanoscale.[1] A wide variety of physical and chemical processes have been explored for the synthesis of metal nanoparticles (NPs).[2–5] Driven by the growing impetus of green chemistry, considerable effort has been put into clean, nontoxic, and environmentally benign biosynthesis of metal NPs, using microorganisms without the need for auxiliary capping agents.[6] Some microorganisms have been used to synthesize several metal NPs *e.g.* Ag,[7,8] Au,[9–13] Pd[14–18] with catalytic activity.[19,20] It is well-known that silver ions are extremely toxic to most microbial cells. However, Klaus *et al.* demonstrated the biological synthesis of silver-based crystals by challenging *Pseudomonas stutzeri* AG259 cells with silver ions.[21] This work therefore created a novel avenue for green synthesis of Ag NPs based on microorganisms. Our previous study also reported the formation of Ag NPs, which was considerably accelerated by the introduction of OH^- ions to the biosynthetic system using dry *Aeromonas sp*. SH10 cells instead of live cells.[22] Similarly, Au and Pd NPs with lower toxicity than Ag NPs have also been synthesized using different kinds of microorganisms. For example, earlier studies suggested that c-type cytochromes of Fe(III)-reducing bacterium *G. metallireducens* were able to transfer electrons to soluble Au(III).[23,24] Afterwards, a wide range of microorganisms such as bacteria[12,25,26] and fungi[10,11,13] have been employed to synthesize Au NPs. Pd which belongs to the platinum group of metals is widely used as an efficient catalyst.[17] In 1998, Macaskie *et al.* first reported that bio-Pd supported by *Desulfovibrio desulfuricans* could be fabricated with the electron donor formate or H_2.[27] Thereafter, several applications of bio-Pd as a catalyst in dehalogenation,[28,29] reduction,[30,16,18] hydrogenation[18,28,31] and C–C bond forming[15,18] reactions have been demonstrated.

In comparison with monometallic NPs, there is an enhancement in specific properties upon alloying with the other metal due to synergistic effect, and the rich diversity of compositions, structures, and properties of metallic alloys leading to widespread applications in electronics, engineering, and catalysis.[32,33] Although metal-microorganism interaction and the consequent formation of biological metal (nano-) precipitates have been described in literature for more than 30 years,[34] microbial biosynthesis of bimetallic NPs has been studied only in recent years,[35–38] *e.g.* Pd/Fe,[38] Au/Pd,[35/37] Ag/Au,[11,39] *etc.* As far as the biosynthesis of Au/Pd NPs was concerned, Corte *et al.*[35] and Hosseinkhani *et al.*[37] reported the microbial synthesis of bimetallic Au/Pd NPs, respectively. Hosseinkhani *et al.* adopted a two-step method to synthesize nearly spherical bimetallic Au/Pd NPs supported over *Cupriavidus necator* H16 with formate as the electron donor

[a]*Environmental Science Research Center, College of the Environment & Ecology, Xiamen University, Xiamen, 361005, P. R. China*
[b]*Department of Chemical and Biochemical Engineering, College of Chemistry and Chemical Engineering, Xiamen University, Xiamen, 361005, P. R. China. E-mail: cola@xmu.edu.cn; Fax: (+86)592-2184822; Tel: (+86) 592-2183088*
[c]*National Engineering Laboratory for Green Chemical Productions of Alcohols, Ethers and Esters, Xiamen University, Xiamen, 361005, P. R. China*
[d]*Key Lab for Chemical Biology of Fujian Province, Xiamen University, Xiamen, 361005, P. R. China*
[e]*The Key Lab for Synthetic Biotechnology of Xiamen City, Xiamen University, Xiamen, 361005, P. R. China*

which showed quite good catalytic activity for the reduction of p-nitrophenol (4-NP), much better than Au NPs and Pd NPs[37]. Nevertheless, Corte *et al.* fabricated nearly spherical Pd/Au NPs supported on *S. oneidensis* bacteria to efficiently catalyze the degradation of diclofenac and trichloroethylene (TCE).[35,40] These composites also showed good catalytic activity on Suzuki coupling reaction in a recent report.[41] In contrast, Deplanche *et al.* synthesized nearly spherical core/shell gold/palladium NPs on *E. coli* by microbially premade Pd seeds, which showed excellent selectivity towards benzaldehyde in solvent-free oxidation of benzyl alcohol without a base at low temperature, outperforming a commercial Pd catalyst.[36,40] Even though the microbial approaches to Au/Pd NPs have been studied, controlling composition and shape of the NPs has been little reported.[37] Moreover, these processes were carried out under specific environmental conditions (degassing by N_2, vacuum and anaerobic condition) and most of the NP structures were not sufficiently characterized.[36,37] By far, the only STEM study on configuration of microbially synthesized Au/Pd NPs by *Desulfovibrio desulfuricans* was carried out by Tran *et al.*[32]

In this study, Au/Pd NPs were synthesized by the eukaryotic organism, *Pichia pastoris* (*P. pastoris*) GS115, in the presence of H_2 without the need of using any specific environment (degassing by N_2, vacuum and anaerobic condition), leading to Au/Pd alloy NP/*P. pastoris* composites. The effects of the biosynthetic conditions, including the type of solution, the molar ratio of Au/Pd, the concentration of Cl^-, the pre-adsorption time and the nature of the yeast used, on the composition of the alloy NPs were studied. Furthermore, the bimetallic Au/Pd alloy structures were characterized by various techniques such as transmission electron microscopy (TEM), scanning transmission electron microscopy (STEM), energy dispersive X-ray (EDX) and X-ray photoelectron spectroscopy (XPS) analyses. Interestingly, flower-like Au/Pd alloy NP/*P. pastoris* composites were successfully fabricated for the first time and the composition was controlled by adjusting the initial molar ratio of the precursors.

2. Materials and methods

2.1 Materials and reagents

Pichia pastoris GS115 was purchased from Invitrogen Corporation, USA. Chloroauric acid ($HAuCl_4$), palladium chloride ($PdCl_2$), glutaraldehyde solution (25%), sodium chloride (NaCl) and 3-(*N*-morpholino)propanesulphonic acid-NaOH (MOPS-NaOH) buffer were all purchased from Sinopharm Chemical Reagent Co., Ltd. in China. Deionized (DI) water was used throughout the work.

2.2 Yeast strains and growth conditions

Pichia pastoris GS115 yeast were grown in YPD nutrient broth (20 g L^{-1} glucose, 20 g L^{-1} soya peptone and 10 g L^{-1} yeast) at 30 °C and 200 rpm for 48 h.[42] Then the yeast cells were harvested by centrifugation (5000 rpm, 10 min) at room temperature, and then washed thrice with physiological saline (weight/volume ratio: 0.9%). These wet yeast cells of 0.2 g[43] were dissolved in 10 mL solution (OD_{600} 1.0, dried weight 0.04 g) to biosynthesize the NPs. The solution was later diluted with $\times 50$ deionized water before taking UV-vis spectra.

2.3 Preparation of flower-like Au/Pd/*P. pastoris* composites

In a typical biosynthesis for Au/Pd NPs, the carefully weighted wet cells (0.2 g) were resuspended in 10 mL 0.9% (w/v) physiological saline. The solution was hosted in a 50 mL, three-neck flask (contained a Teflon-coated magnetic stirring bar). $PdCl_2$ and $HAuCl_4$ solution were added simultaneously to the cell suspension to obtain the final Pd(II) and Au(III) concentrations of 0.62 and 0.37 mM, respectively. The Pd(II) and Au(III) ions were first adsorbed by the yeast at 30 °C for 15 min. Then H_2 was sparged through the suspension (40 mL min^{-1}, 15 min). Subsequently, the yeast solutions were kept at a temperature of 30 °C for 24 h to form Au/Pd NP/*P. pastoris* composites.

2.4 Characterizations of flower-like Au/Pd/*P. pastoris* composites

The composites harvested by centrifugation after being washed thrice with deionized water, were first immersed in 4% glutaraldehyde solution for 10 min,[37] then washed with DI water. Afterwards, a drop of hydrosol was then deposited on a carbon thin film coating copper grids for TEM observations. TEM observations and EDX analyses were performed on an electron microscope (Tecnai F30, FEI; Netherlands) with an accelerating voltage of 300 kV. After the reaction, the resulting solutions were centrifuged at 6000 rpm for 10 min. Then the precipitates were dried at 50 °C and collected for XPS analysis, which was performed on a Quantum 2000 spectrometer using the Al-Kα line as the excitation source. The binding energy was calibrated using *C*1 s as reference energy (*C*1 s = 284.8 eV). The supernatant solutions were decanted after removing the composites by centrifuging. Thereafter, the Pd(II) and Au(III) concentrations in the solutions were analyzed using atomic absorption spectrophotometer (AAS) (Pgeneral, China).

3. Results and discussion

3.1 Characterization of Au/Pd/*P. pastoris* composites

Fig. 1a shows the TEM image of the *P. pastoris* cells after reacting with the Au and Pd precursors at a concentration of NaCl solution 0.9% (w/v), molar ratio of Au : Pd (1 : 2) and the pre-adsorption time of Au(III) and Pd(II) of 15 min. As shown, there were lots of NPs measuring tens of nanometers over the cell surface. The TEM images of the NPs at higher magnification (Fig. 1b and Fig. 1c) revealed that they were flower-like in shape. EDX elemental line scanning on a single NP (Fig. 1d) showed that, they were composed of Au and Pd, preliminarily showing their bimetallic nature. The bimetallic nanostructures of Au/Pd were further validated by STEM observation and elemental mapping. The STEM image of the Au/Pd NPs is given in Fig. 2a, showing that there were plenty of well-defined NPs. The elemental mapping images of these NPs further verify that most of the Au (yellow, Fig. 2b) and Pd atoms

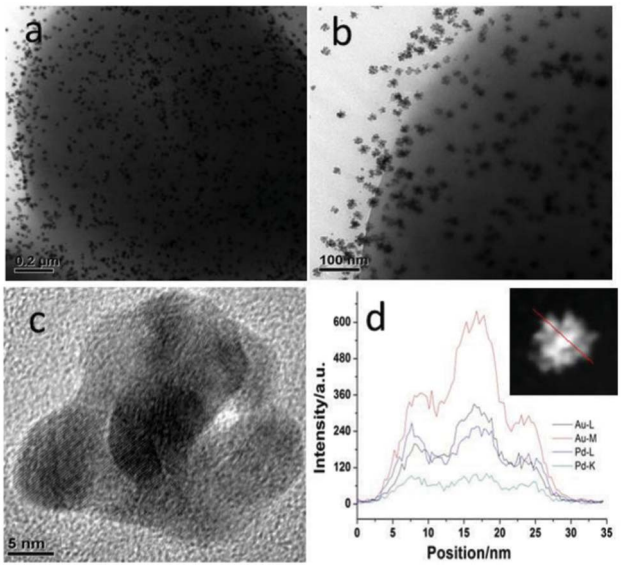

Fig. 1 TEM images of Au/Pd/*P. pastoris* composites in physiological saline (a–c) and cross-sectional compositional line profiles of bimetallic NP (d). (Synthesis conditions: 30 °C, 0.9% (w/v) physiological saline, Au(III) concentration of 0.37 mM, Pd(II) concentration of 0.62 mM, H_2 by bubbling 40 mL min^{-1} for 15 min, adsorption time of 15 min, 24 h.)

(orange, Fig. 2c) were homogeneously distributed over the entire NP structures. The compositions of these bimetallic NPs were confirmed by EDX measurement over micro-regions. The results showed that the compositions were close to the initial molar ratio of Au to Pd. The compositions of the Au/Pd NPs and the surface valence states of the metals were measured by XPS. Fig. 3 shows XPS spectra of Pd 3d peaks (a) and Au 4f peaks (b) on the Au/Pd/*P. pastoris* composites. The Pd (0) 3d spectrum consists of doublet peaks of the $3d_{5/2}$ and $3d_{3/2}$. Fig. 3a shows that, the 335.7 eV was that of the Pd (0) $3d_{5/2}$ peak, a weak shift to higher binding energies by 0.2–0.4 eV according to the ref. 44, 45. The $3d_{3/2}$ peak doublet shifted 5.25 eV with respect to the $3d_{5/2}$ peak. The weak Pd(II) 3d peak was also shown in the Fig. 3a as some Pd atoms on the cell surface were oxidized by air to some extent. Furthermore, Fig. 3b shows the peak of Au(0) $4f_{7/2}$. It can be determined by XPS analysis,[46] that the atomic ratio of Au/Pd in the bimetallic Au/Pd alloy NPs was 1 : 2, which was also consistent with the initial molar ratio of Au/Pd. According to the AAS results, there were no residual Pd(II) and Au(III) ions in the solution. That is to say, all the Pd(II) and Au(III) ions were adsorbed on the cell

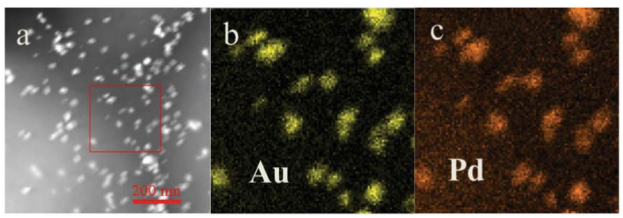

Fig. 2 STEM image of Au/Pd/*P. pastoris* composites in HADDF (a); EDX elemental maps of Au (b) and Pd (c) concentrations in the NPs.

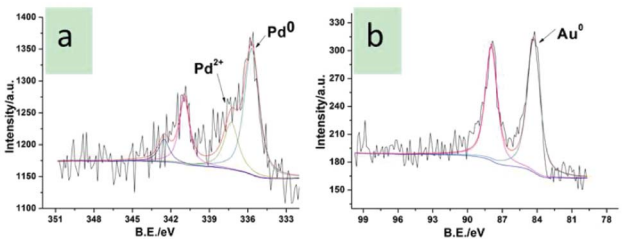

Fig. 3 XPS of the Pd 3d peaks (a) and the Au 4f peaks (b) on the biosynthesized Au/Pd/*P. pastoris* composites.

surface and totally reduced to form the Au/Pd alloy NPs. Next, comparative experiments were conducted to investigate the effect of the solvent type, the initial molar ratio of the two precursors, Cl^- concentration, pre-adsorption time, and pretreatment of the *P. pastoris* cells on the morphology and composition of the NPs.

3.2 Effect of the synthetic conditions

3.2.1 Effect of the solvent. In previous studies, Au/Pd NPs were microbially reduced in MOPS-NaOH buffer[36] or DI water.[32,35] The medium was first considered in this work. Similarly, Au/Pd NP/*P. pastoris* composites were also synthesized in DI water and MOPS-NaOH buffer instead of physiological saline. As shown in Fig. 4, some NPs agglomerated slightly in DI water and the morphology was not uniform (Fig. 4a), while spherical particles were dispersed on the cell surface in the biological buffer (Fig. 4c). Even though the same flower-like NPs could not be obtained, EDX elemental line from a single particle (Fig. 4b) and EDX spectrum (Fig. 4d) confirmed that the nanostructures were still bimetallic. The different shapes may be attributed to the ions in the solution.

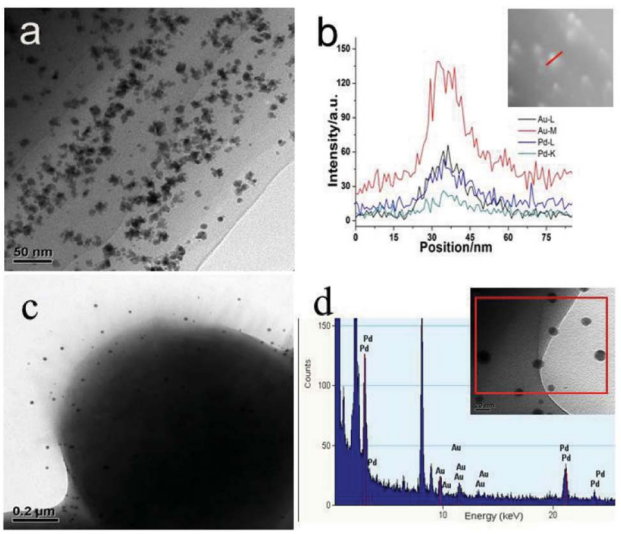

Fig. 4 TEM image of Au/Pd/*P. pastoris* composites (a) and cross-sectional compositional line profiles of bimetallic NP (b) in DI water; TEM image (c) and EDX spectrum (d) in MOPS-NaOH buffer. (Synthesis conditions: 30 °C, Au(III) concentration of 0.37 mM, Pd(II) concentration of 0.62 mM, H_2 by bubbling 40 mL min^{-1} for 15 min, adsorption time of 15 min, 24 h.)

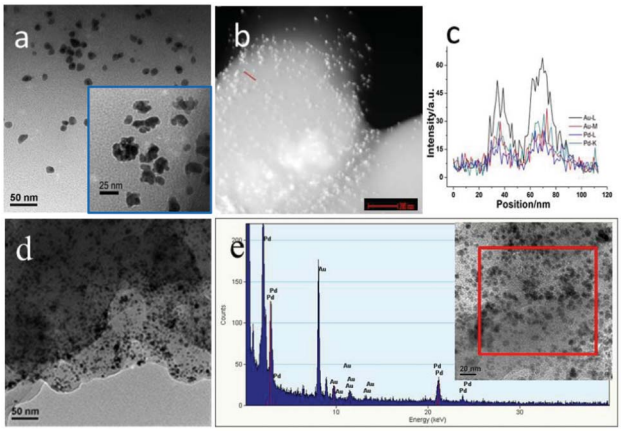

Fig. 5 TEM image (a), STEM image (b) and cross-sectional compositional line profiles (c) of Au/Pd/*P. pastoris* composites in 0.45% (w/v) NaCl solution and TEM image (d), EDX spectrum (e) of Au/Pd/*P. pastoris* composites in 1.35% NaCl solution. (Synthesis conditions: 30 °C, Au(III) concentration of 0.37 mM, Pd(II) concentration of 0.62 mM, respectively, H_2 by bubbling of 40 mL min^{-1} for 15 min, adsorption time of 15 min, 24 h.)

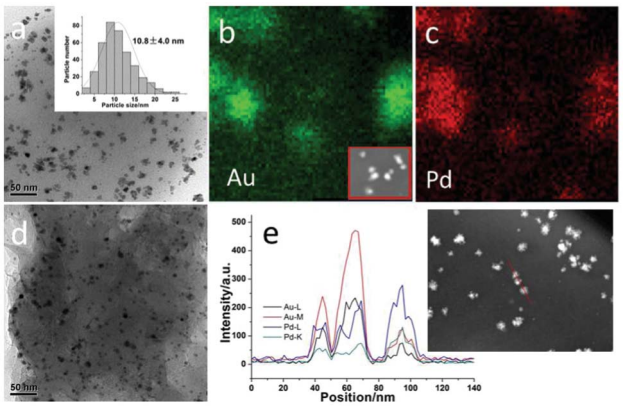

Fig. 6 TEM image (a), EDX elemental maps of Au (b) and Pd (c) concentrations in the Au/Pd NPs (molar ratio 1 : 1); TEM image (d) and cross-sectional compositional line profiles of bimetallic Au/Pd NPs (e) (molar ratio 2 : 1). (Synthesis conditions: 30 °C, 0.9% (w/v) physiological saline, H_2 by bubbling of 40 mL min^{-1} for 15 min, adsorption time of 15 min, 24 h.)

There were no anions (Cl^-) in MOPS-NaOH buffer or in DI water, compared with physiological saline. And flower-like NPs were not obtained in these two solutions. Thus, the factor of Cl^- concentration was discussed next.

3.2.2 Effect of the Cl^- concentration. Physiological saline, 0.9% (w/v) NaCl, was employed in order to keep the *P. pastoris* cells intact. However, the synthesis of the NPs was also affected by Cl^-. When the concentration of Cl^- was 0.45% (w/v), some flower-like aggregates could be observed though some nearly spherical NPs were also produced (Fig. 5a–b). In contrast, when the concentration of Cl^- was 1.35% (w/v), the NPs were nearly spherical but the size was much smaller (Fig. 5d). EDX elemental line scanning on a single particle (Fig. 5c) and EDX spectrum (Fig. 5e) confirmed that the NPs on the cell surface were also composed of two metal elements. Interaction of Cl^- with Au and Pd was discussed in the previous studies, respectively.[47,48] Herein, however, the mechanism on how Cl^- affected the shape of the Au/Pd alloy NPs remained unanswered as it was complicated in the $HAuCl_4/PdCl_2$/*P. pastoris*/NaCl system. Cl^- not only affected the growth of both Au and Pd nuclei, but also had an influence on the surface property of the *P. pastoris* cells which also affected the growth of the NPs. It has been shown in literature that high Cl^- concentrations was detrimental to anisotropic growth of Au nanocrystals[47] while chemisorption or surface coordination of Cl^- on Pd was not strong.[48] Therefore, anisotropic NPs were suppressed when the Cl^- concentration was 1.35% (w/v).

3.2.3 Effect of the initial molar ratio of Au to Pd. The atomic ratio of Au to Pd in the above flower-like NPs was nearly 1 : 2 and in good agreement with the initial molar ratio of the precursors. However, if different initial molar ratios were adopted, the obtained structure should be further studied. Controlled experiments were carried out for Au/Pd molar ratios of 1 : 1 and 2 : 1, besides 1 : 2 discussed above. When the molar ratio of Au : Pd was altered to 1 : 1, very small NPs and petal-like NPs were obtained, with both dispersed uniformly on the cell surface (Fig. 6a). Their size varied from several nm to dozens of nm (10.8 ± 4.0 nm) and the relative standard deviation (R.S.D.) was 37%. These very small NPs seemed to be Pd NPs as it was much easier for Pd atoms to form small NPs than Au atoms. Nevertheless, these NPs could not assemble with Au NPs to form the flower-like shape. The compositions of some spherical NPs over a micro-region were verified by STEM images (Fig. 6b–c). These colored elemental mapping images proved that the Au (green, Fig. 6b) and Pd atoms (red, Fig. 6c) were uniformly distributed over the NPs structure, *i.e.* some NPs structures were still alloy under these conditions. When the molar ratio of Au : Pd was increased to 2 : 1, the resulting NPs were with irregular shapes and the sizes of the nearly spherical NPs became smaller (8.1 ± 1.8 nm) (Fig. 6d). And the R.S.D was only 22%, indicating a narrower size distribution. EDX elemental line scanning (Fig. 6e) on three NPs confirms that the NPs were composed of Au and Pd. Even though these particles with irregular shape under these two conditions were no longer flower-like in shape, the particles were still alloy. Compared with the flower-like shape at molar ratio of Au : Pd of 1 : 2, it seems that when the molar ratio of Pd to Au was higher, there were enough Pd atoms to assemble with Au atoms to form the flower-like nanostructures. Thus, the initial molar ratio of Au to Pd had a significant effect on the shape of the alloy NPs.

3.2.4 Effect of the pre-adsorption time. It has been well documented that, some cells could adsorb and reduce some metal ions to atoms. Therefore, the pre-adsorption time before sparging H_2 could affect the metallic nucleation site. Fig. 7a shows NPs with similar flower-like morphology located on the cell surface when pre-adsorption time was prolonged to 30 min. However, when the pre-adsorption time increased to 60 min, the morphology of the NPs was nearly spherical (Fig. 7c). Fig. 7b and d show distributions of Au and Pd along the cross-sectional line profiles of the Au/Pd NPs. If H_2 were directly sparged through solution together with the two kinds of metal ions, it worked as a strong reducing agent that can easily

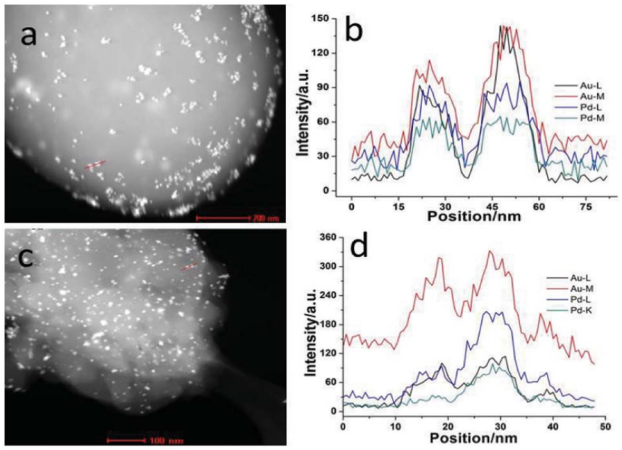

Fig. 7 STEM images and cross-sectional compositional line profiles of bio-synthesized Au/Pd/*P. pastoris* composites after pre-adsorption time of 30 min (a–b) and 60 min (c–d). (Synthesis conditions: 30 °C, 0.9% (w/v) physiological saline, Au(III) concentration of 0.37 mM, Pd(II) concentration of 0.62 mM, H_2 by bubbling of 40 mL min^{-1} for 15 min, 24 h.)

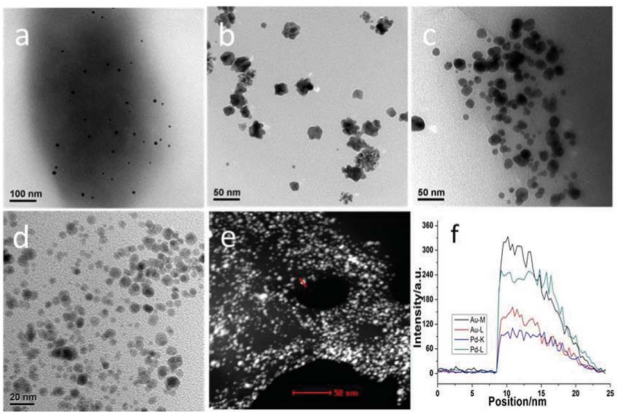

Fig. 8 TEM images of biosynthesized Au/Pd nanoparticles over stale yeast (a–c) and dried yeast (d, e) was taken by STEM and f was one of cross-sectional compositional line profiles of bimetallic NP in the yeast. (Synthesis conditions: 30 °C, 0.9% (w/v) physiological saline, Au(III) concentration of 0.37 mM, Pd(II) concentration of 0.62 mM, H_2 by bubbling of 40 mL min^{-1} for 15 min, adsorption time of 15 min, 24 h.)

reduce the two metal ions. As a result, the NPs were well dispersed in the solution beyond the cells. The metal ions may be adsorbed and reduced by the cells only. However, they cannot be completely reduced without H_2 as electron donor, especially the Pd(II) ions. Hence, such alloy NPs described above cannot be obtained. To fabricate the Au/Pd alloy NPs over *P. pastoris* cells, the two kinds of metal ions should be pre-adsorbed by the yeast for some time prior to blowing of H_2. In other words, the yeast was able to reduce the metal ions in the presence of electron donor H_2. It was generally accepted that hydrogenases of the cells, after charging with electron donor of H_2 or formate, functioned as nucleation site and initialized the Pd or Au reduction.[17,49] Subsequently, Pd(II) and Au(III) were autocatalytically reduced on these nuclei. The longer the pre-adsorption time, the more the adsorbed ions on the cell surface. Consequently, more nuclei were obtained, favouring the growth of the bimetallic NPs.

3.2.5 Effect of the nature of the yeast. The nature of the yeast had an effect on the formation of the bimetallic NPs, since they (bimetallic NPs) were synthesized on the cell surface. Therefore, controlled experiments were carried out to identify the effect of the nature of the yeast used on the property of the NPs. In one experiment stale yeast, kept in a refrigerator (4 °C) for at least one week was used, while in the other yeast, dried yeast kept at 50 °C for 24 h was employed. In Fig. 8a–c, it seemed that only a few NPs on the cell surface were observed in the case of the stale yeast, as it lacked adsorption ability, with the obtained NPs not evenly dispersed and irregular in shapes. These may be attributed to the slight fermentation and the change in protease or others on the surface of *P. pastoris*. However, the EDX measurement over micro-region showed that there were Au and Pd metals on the cell surface. In contrast, spherical Au/Pd NPs were obtained (Fig. 8d–e) on the surface if dried yeast cells[50,51] were adopted. In addition the reaction conditions had to be changed, *i.e.* increasing the temperature to 60 °C and sweeping the headspace of the reaction solution by H_2. EDX elemental line scanning on a single particle (Fig. 8f) indicated that the NPs were also composed of two kinds of elements, Au and Pd. Therefore, Au/Pd alloy NPs could also be synthesized using dead yeast but the resulting shape was no longer flower-like.

3.3 Formation mechanism of flower-like Au/Pd NPs

Obviously, alloy NPs with varied morphologies were synthesized under different conditions using *P. pastoris* cells and H_2. During H_2 sparging, the color of the solution firstly went from yellow to pink, indicating the reduction of cell surface-bound Au(III) into Au(0) at the beginning. Then, with time going on, the color of the solution changed from pink to dark, indicating the reduction of Pd(II) to Pd(0). To clarify the formation mechanism of the alloy NPs, it is reasonable to suggest that the Au atoms on the surface of the yeast are preferentially located in the ''pistil'' region, while the Pd atoms are preferentially located in the ''petals'' region, since the reduction potentials of Au ions are more positive than those of Pd ions (E^0 ($[PdCl_4]^{2-}/Pd^0$) = +0.59 V,[33] E^0 ($[AuCl_4]^-/Au^0$) = +0.93 V *vs.* NHE).[52] As the reaction progresses, the deposited surface Pd atoms mixes with the Au atoms through the process of interdiffusion[53] during the next 24 h, eventually resulting in the formation of homogeneous Au/Pd alloy NPs on the surface of the yeast cells. The formation mechanism of the flower-like Au/Pd alloy NPs could be described as in Fig. 9. Firstly, Au atoms were located on the cell surface, then Pd atoms aggregated on the surface of Au atoms. Afterwards, part of the Au atoms were replaced by Pd atoms and Au/Pd atoms assembled homogeneously distributed over the entire flower-like alloy nanostructures through interdiffusion process[53] (Fig. 2).

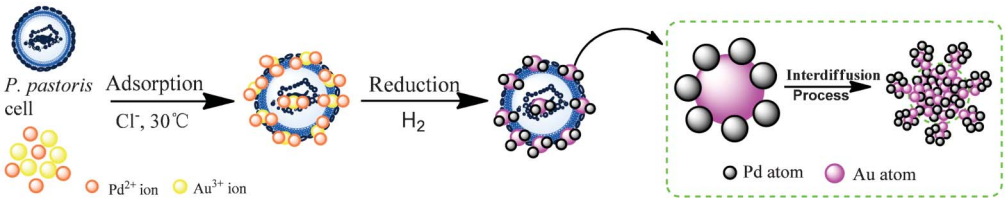

Fig. 9 Schematic illustration of formation mechanism of flower-like Au/Pd alloy NP/*P. pastoris* composites.

4. Conclusions

In conclusion, Au/Pd alloy NP/*Pichia pastoris* composites were synthesized under the following different reaction conditions, types of solvent, molar ratio of Au/Pd, concentration of Cl^-, pre-adsorption time and nature of the yeast used. The alloy nanostructures were confirmed by EDX elemental line scanning on the NPs and STEM mapping. Interestingly, flower-like alloy Au/Pd NP/*P. pastoris* composites were successfully fabricated under the following reaction conditions, concentration of NaCl solution 0.9% (w/v), molar ratio of Au/Pd (1 : 2) and 15 min pre-adsorption of Au(III) and Pd(II) ions through fresh yeast reduction in the presence of H_2. STEM images and EDX elemental line scanning results showed that the two kinds of metals were well distributed in the NPs. According to EDX and XPS measurement, the compositions of the flower-like Au/Pd NPs could be effectively controlled by adjusting the initial molar ratio of Au/Pd. This work exemplifies an effectual means of controlling the composition of the Au/Pd alloy NPs and synthesizing flower-like Au/Pd alloy NPs over microbial cells.

Acknowledgements

This work was supported by the Fundamental Research Funds for Central Universities (No.2010121051) and the NSFC projects (Nos.21106117 and 21036004).

Notes and references

1 R. Coppage, J. M. Slocik, B. D. Briggs, A. I. Frenkel, H. Heinz, R. R. Naik and M. R. Knecht, *J. Am. Chem. Soc.*, 2011, **133**, 12346–12349.
2 S. J. Guo and E. K. Wang, *Nano Today*, 2011, **6**, 240–264.
3 C. Vollmer and C. Janiak, *Coord. Chem. Rev.*, 2011, **255**, 2039–2057.
4 X. S. Wang, D. P. Yang, P. Huang, M. Li, C. Li, D. Chen and D. X. Cui, *Nanoscale*, 2012, **4**, 7766–7772.
5 B. Wu and N. Zheng, *Nano Today*, 2013, **8**, 168–197.
6 O. V. Kharissova, H. Dias, B. I. Kharisov, B. O. Pérez and V. M. J. Pérez, *Trends Biotechnol.*, 2013, **31**, 240–248.
7 M. Kowshik, S. Ashtaputre, S. Kharrazi, W. Vogel, J. Urban, S. K. Kulkarni and K. M. Paknikar, *Nanotechnology*, 2003, **14**, 95–100.
8 B. Despax, C. Saulou, P. Raynaud, L. Datas and M. Mercier-Bonin, *Nanotechnology*, 2011, **22**, 175101.
9 Y. Y. Liu, J. K. Fu, H. B. Hu, D. L. Tang, Z. Y. Lin, Z. M. Ni and X. S. Yu, *Chin. Sci. Bull.*, 2001, **46**, 1179–1182.
10 R. Bhambure, M. Bule, N. Shaligram, M. Kamat and R. Singhal, *Chem. Eng. Technol.*, 2009, **32**, 1036–1041.
11 E. Castro-Longoria, A. R. Vilchis-Nestor and M. Avalos-Borja, *Colloids Surf., B*, 2011, **83**, 42–48.
12 M. I. Husseiny, M. A. El-Aziz, Y. Badr and M. A. Mahmoud, *Spectrochim. Acta, Part A*, 2007, **67**, 1003–1006.
13 X. R. Zhang, X. X. He, K. M. Wang, Y. H. Wang, H. M. Li and W. H. Tan, *J. Nanosci. Nanotechnol.*, 2009, **9**, 5738–5744.
14 P. Yong, N. A. Rowson, J. P. G. Farr, I. R. Harris and L. E. Macaskie, *J. Chem. Technol. Biotechnol.*, 2002, **77**, 593–601.
15 L. S. Søbjerg, D. Gauthier, A. T. Lindhardt, M. Bunge, K. Finster, R. L. Meyer and T. Skrydstrup, *Green Chem.*, 2009, **11**, 2041–2046.
16 D. Chidambaram, T. Hennebel, S. Taghavi, J. Mast, N. Boon, W. Verstraete, D. van der Lelie and J. P. Fitts, *Environ. Sci. Technol.*, 2010, **44**, 7635–7640.
17 T. Hennebel, S. D. Corte, W. Verstraete and N. Boon, *Curr. Opin. Biotechnol.*, 2012, **23**, 555–561.
18 L. S. Søbjerg, A. T. Lindhardt, T. Skrydstrup, K. Finster and R. L. Meyer, *Colloids Surf., B*, 2011, **85**, 373–378.
19 J. R. Lloyd, *FEMS Microbiol. Rev.*, 2006, **27**, 411–425.
20 M. Sastry, A. Ahmad, M. I. Khan and R. Kumar, *Curr. Sci.*, 2003, **85**, 162–170.
21 T. Klaus, R. Joerger, E. Olsson and C. G. Granqvist, *Proc. Natl. Acad. Sci. U. S. A.*, 1999, **96**, 13611–13614.
22 H. X. Wang, H. M. Chen, Y. Wang, J. L. Huang, T. Kong, W. S. Lin, Y. Zhou, L. Lin, D. H. Sun and Q. B. Li, *Curr. Nanosci.*, 2012, **8**, 838–846.
23 J. R. Lloyd, *FEMS Microbiol. Rev.*, 2003, **27**, 411–425.
24 D. R. Lovley, S. J. Giovannoni, D. C. White, J. E. Champine, E. Phillips, Y. A. Gorby and S. Goodwin, *Arch. Microbiol.*, 1993, **159**, 336–344.
25 K. Kalishwaralal, V. Deepak, S. R. K. Pandian, M. Kottaisamy, S. BarathManiKanth, B. Kartikeyan and S. Gurunathan, *Colloids Surf., B*, 2010, **77**, 257–262.
26 K. Deplanche, R. D. Woods, I. P. Mikheenko, R. E. Sockett and L. E. Macaskie, *Biotechnol. Bioeng.*, 2008, **101**, 873–880.
27 J. R. Lloyd, P. Yong and L. E. Macaskie, *Appl. Environ. Microbiol.*, 1998, **64**, 4607–4609.
28 N. J. Creamer, K. Deplanche, T. J. Snape, I. P. Mikheenko, P. Yong, D. Samyahumbi, J. Wood, K. Pollmann, S. Selenska-Pobell and L. E. Macaskie, *Hydrometallurgy*, 2008, **94**, 138–143.
29 I. P. Mikheenko, M. Rousset, S. Dementin and L. E. Macaskie, *Appl. Environ. Microbiol.*, 2008, **74**, 6144–6146.

30 A. N. Mabbett, D. Sanyahumbi, P. Yong and L. E. Macaskie, *Environ. Sci. Technol.*, 2006, **40**, 1015–1021.
31 J. Wood, L. Bodenes, J. Bennett, K. Deplanche and L. E. Macaskie, *Ind. Eng. Chem. Res.*, 2010, **49**, 980–988.
32 D. T. Tran, I. P. Jones, J. A. Preece, R. L. Johnston, K. Deplanche and L. E. Macaskie, *Nanotechnology*, 2012, **23**, 055701.
33 S. Iravani, *Green Chem.*, 2011, **13**, 2638–2650.
34 G. M. Gadd, *Microbiology*, 2010, **156**, 609–643.
35 S. D. Corte, T. Hennebel, J. P. Fitts, T. Sabbe, V. Bliznuk, S. Verschuere, D. van der Lelie, W. Verstraete and N. Boon, *Environ. Sci. Technol.*, 2011, **45**, 8506–8513.
36 K. Deplanche, M. L. Merroun, M. Casadesus, D. T. Tran, I. P. Mikheenko, J. A. Bennett, J. Zhu, I. P. Jones, G. A. Attard and J. Wood, *J. R. Soc. Interface*, 2012, **9**, 1705–1712.
37 B. Hosseinkhani, L. S. Søbjerg, A. E. Rotaru, G. Emtiazi, T. Skrydstrup and R. L. Meyer, *Biotechnol. Bioeng.*, 2012, **109**, 45–52.
38 *Geneva, Switzerland Pat.*, WO2011141418A1, 2011.
39 S. Senapati, A. Ahmad, M. I. Khan, M. Sastry and R. Kumar, *Small*, 2005, **1**, 517–520.
40 K. Deplanche, I. P. Mikheenko, J. A. Bennett, M. Merroun, H. Mounzer, J. Wood and L. E. Macaskie, *Top. Catal.*, 2011, **54**, 1110–1114.
41 T. S. A. Heugebaert, C. S. De, T. Sabbe, T. Hennebel, W. Verstraete, N. Boon and C. V. Stevens, *Tetrahedron Lett.*, 2012, **53**, 1410–1412.
42 L. Lin, W. Wu, J. Huang, D. Sun, N. u. M. Waithera, Y. Zhou, H. Wang and Q. Li, *Chem. Eng. J.*, 2013, **225**, 857–864.
43 S. K. Srivastava and M. Constanti, *J. Nanopart. Res.*, 2012, **14**, 1–10.
44 M. Bunge, L. S. Søbjerg, A. E. Rotaru, D. Gauthier, A. T. Lindhardt, G. Hause, K. Finster, P. Kingshott, T. Skrydstrup and R. L. Meyer, *Biotechnol. Bioeng.*, 2010, **107**, 206–215.
45 V. S. Coker, J. A. Bennett, N. D. Telling, T. Henkel, J. M. Charnock, G. van der Laan, R. A. D. Pattrick, C. I. Pearce, R. S. Cutting and I. J. Shannon, *ACS Nano*, 2010, **4**, 2577–2584.
46 M. L. Wu, D. H. Chen and T. C. Huang, *Langmuir*, 2001, **17**, 3877–3883.
47 J. S. DuChene, W. Niu, J. M. Abendroth, Q. Sun, W. Zhao, F. Huo and W. D. Wei, *Chem. Mater.*, 2012, **25**, 1392–1399.
48 A. Carrasquillo Jr, J.-J. Jeng, R. J. Barriga, W. F. Temesghen and M. P. Soriaga, *Inorg. Chim. Acta*, 1997, **255**, 249–254.
49 W. D. Windt, P. Aelterman and W. Verstraete, *Environ. Microbiol.*, 2005, **7**, 314–325.
50 M. Wang, T. Kong, X. Jing, Y.-K. Hung, D. Sun, L. Lin, Y. Zheng, J. Huang and Q. Li, *Ind. Eng. Chem. Res.*, 2012, **51**, 16651–16659.
51 M. Wang, T. Odoom-Wubah, H. Chen, X. Jing, T. Kong, D. Sun, J. Huang and Q. Li, *Nanoscale*, 2013, **5**, 6599–6606.
52 K. Fuku, T. Sakano, T. Kamegawa, K. Mori and H. Yamashita, *J. Mater. Chem.*, 2012, **22**, 16243–16247.
53 Y. Ding, F. R. Fan, Z. Q. Tian and Z. L. Wang, *J. Am. Chem. Soc.*, 2010, **132**, 12480–12486.